Towards a Sharper Picture of R136 with SPHERE Extreme Adaptive Optics

Zeinab Khorrami[1,2]
Farrokh Vakili[1]
Thierry Lanz[1]
Maud Langlois[3,4]
Eric Lagadec[1]
Michael R. Meyer[5,6]
Raffaele Gratton[7]
Jean-Luc Beuzit[8]
David Mouillet[8]

[1] School of Physics and Astronomy, Cardiff University, United Kingdom
[2] Université Côte d'Azur, OCA, CNRS, Lagrange, France
[3] Université de Lyon, Université Lyon 1, CNRS, CRAL UMR5574, Saint-Genis Laval, France
[4] Université Aix Marseille, CNRS, Laboratoire d'Astrophysique de Marseille, UMR 7326, France
[5] Institute for Astronomy, ETH Zurich, Switzerland
[6] Department of Astronomy, University of Michigan, Ann Arbor, U.S.A.
[7] INAF — Astronomical Observatory of Padua, Italy
[8] Université Grenoble Alpes, CNRS, Institut de Planétologie et d'Astrophysique de Grenoble, France

The SPHERE extreme adaptive optics instrument was used to observe the central core of the Large Magellanic Cloud, R136, in the near-infrared. This challenging observation demonstrated the capabilities of SPHERE for imaging distant clusters. More than one thousand sources have been detected in Ks- and J-band images in the small field of view of IRDIS covering almost 2.7 × 3.1 pc of the core of R136. Based on isochrone fitting of the colour-magnitude diagram, ages of 1 and 1.5 Myr for the inner 3-arcsecond core and the outer core of R136 fit our data best. The mass function slope is −0.96 ± 0.22 over the mass range of 3 to 300 $M_\odot$. Using SPHERE data, we have gone one step further in partially resolving the core of R136, but this is certainly not the final step and higher resolution is still required.

30 Doradus, in the Large Magellanic Cloud (LMC), is one of the most massive and optically brightest H II regions in the Local Group. In the heart of 30 Doradus, the most massive and compact star cluster R136 is located. This cluster hosts the most massive stars known in the Local Universe (Crowther et al., 2016; Crowther et al., 2010). R136 provides a unique opportunity to study the formation of massive stars and their feedback on cluster formation and evolution.

We used the second-generation Very Large Telescope (VLT) SpectroPolari-metric High-contrast Exoplanet REsearch (SPHERE) instrument to observe the central core of R136 in the near-infrared. Using the small field of view (FoV) of the SPHERE InfraRed Dual-band Imager and Spectrograph (IRDIS), more than one thousand sources have been detected in Ks- and J-band data in the core of R136 (10.9 × 12.3 arcseconds) covering almost 2.7 x 3.1 pc at the distance of R136 (50 kpc).

SPHERE's extreme adaptive optics (AO) system results in the same resolution with the VLT Melipal telescope in the Ks-band as the Hubble Space Telescope (HST) yields in the visible (0.055 arcseconds). In the J-band the resolution of 0.035 arcseconds exceeds that of the HST, and does so with a better pixel sampling of 12.25 milli-arcseconds per pixel.

Observations

We collected data in Guaranteed Time Observation (GTO) runs to image R136 using the classical imaging mode of IRDIS (Langlois et al., 2014). Observations were performed in September 2015, with high dynamic and high angular resolution imaging in J- and Ks-bands, over a FoV of 10.9 × 12.3 arcseconds, centred on the core of the cluster (Figure 1). The seeing was 0.63 ± 0.1 arcseconds during the observations and the night was rated as clear. Less than 10 % of the sky (above 30 degree elevation) was covered by clouds, and the transparency variations were lower than 10 %.

The SPHERE data consist of 300 frames, each of 4.0 s exposure, in the two IRDIS broad-band Ks and J filters (BB-Ks, BB-J). The Wolf-Rayet star R136a1 was used to guide the AO loop of SPHERE, confirming its better-than-nominal performance that surpasses previous NAOS-CONICA (NACO) and Multi-conjugate Adaptive optics Demonstrator (MAD) observations. The air mass during these observations ranged from 1.54 to 1.67. The average Strehl ratio (SR) in the J- and Ks-bands was determined to be 0.40 ± 0.05 and 0.75 ± 0.03, respectively.

In order to qualify our data, we compared the reduced Ks-band images with published images of R136 from HST (with the Wide Field Planetary Camera 3, WFC3) in the V-band and with the MAD imaging (Campbell et al., 2010) in the Ks-band (Figure 2). This comparison confirms that our data present better spatial resolution and point-spread function (PSF) sampling which are more suitable for applying deconvolution techniques. For the photometry, we used the Starfinder package (Diolaiti et al., 2000), implemented in the Interactive Data Language (IDL). Starfinder is designed for the analysis of AO images of crowded fields such as the Galactic Centre (Pugliese et al., 2002). It enables determination of the empirical local PSF from several isolated sources in the image and uses this PSF to extract other stellar sources across the FoV.

Three well-isolated stars (no neighbours within 0.47 arcseconds) were used to extract the PSF in the J- and Ks-band data separately. The extracted PSFs from the J- and Ks-band data were used as input for the stellar source detection by Starfinder. The full width half maximum (FWHM) of the extracted PSFs are 54.71 and 65.16 milli-arcseconds in the J- and Ks-band data, respectively. As a consequence, 1110 and 1059 sources were detected in the J- and Ks-bands, respectively, with a signal-to-noise ratio (S/N) better than two. The AO correction efficiency degrades as a function of distance from R136a1, which is the reference star for the AO loop. At the borders of the FoV, the isoplanatic limits are approached. Overall, the PSF is not centro-symmetric at large distances from R136a1. We took these distortions into account to estimate the local statistical errors, which become significant for those sources that are more distant from the centre of the image than typically 3 arcseconds.
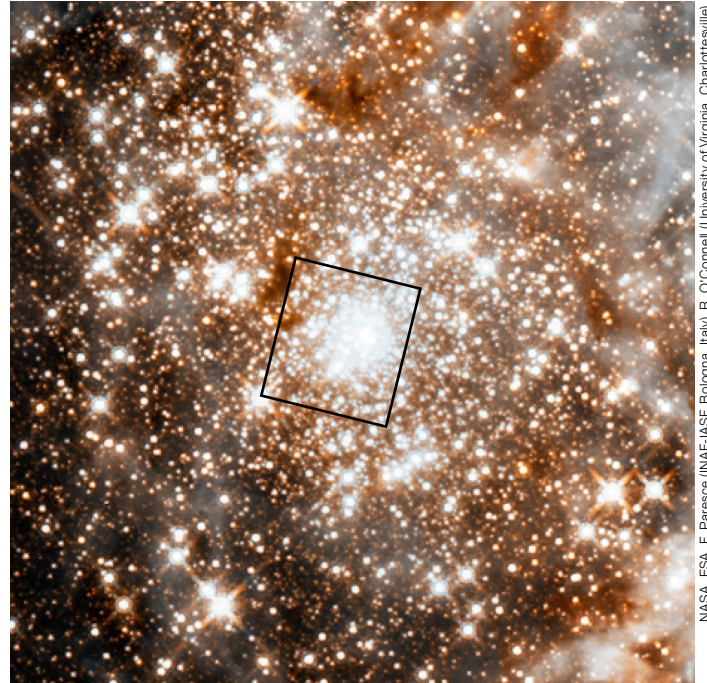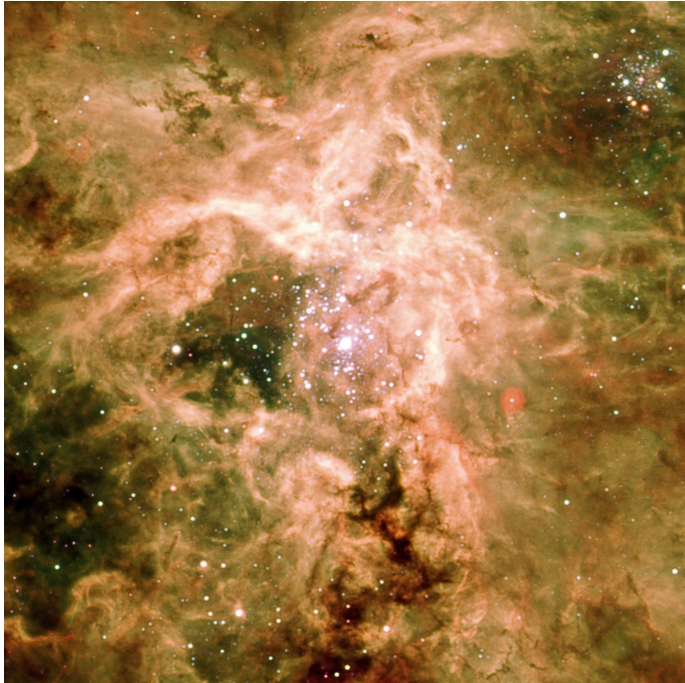
Figure 1. (Upper left) Zooming into the core of R136 (275 arcseconds), from a large-field *BVR* image with FORS1 to the core of R136 (upper right) from an HST WFC3 *JH*-band image (59 arcsecond field-of-view), showing the area imaged by SPHERE IRDIS.

Figure 2. (Lower) Comparison of images of the R136 core with the highest available angular resolution. The FoV of all the images in the upper row is the same as the IRDIS data (10.9 × 12.3 arcseconds);

the lower row of images are zoomed into the very core of R136 (FoV of 1.5 × 1.5 arcseconds). From left to right: HST/WFC3 (*V*-band), MAD (*Ks*-band), and SPHERE/IRDIS (*Ks*-band).
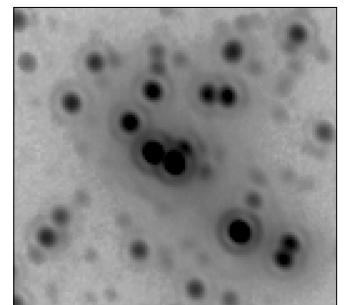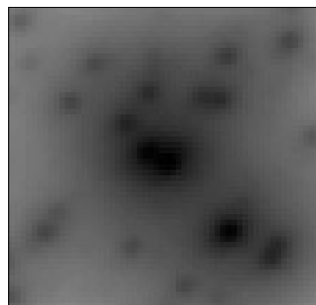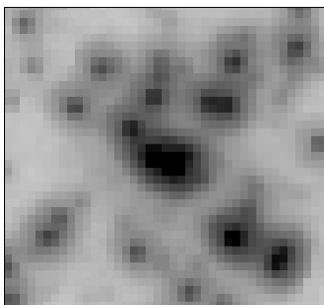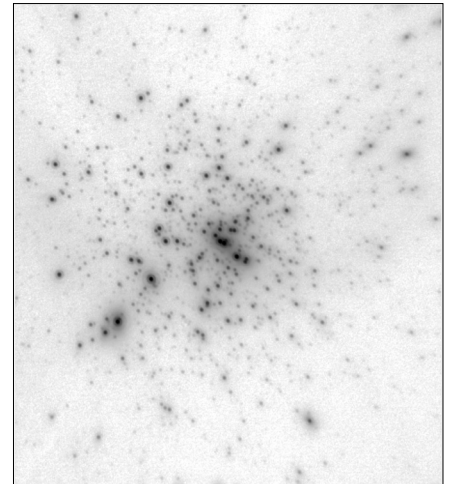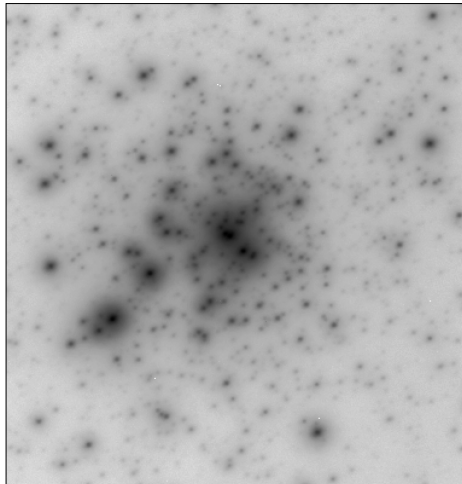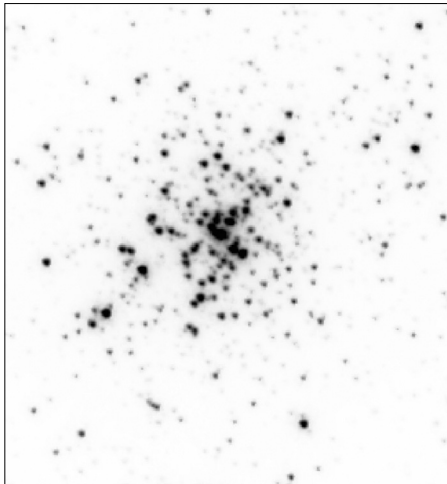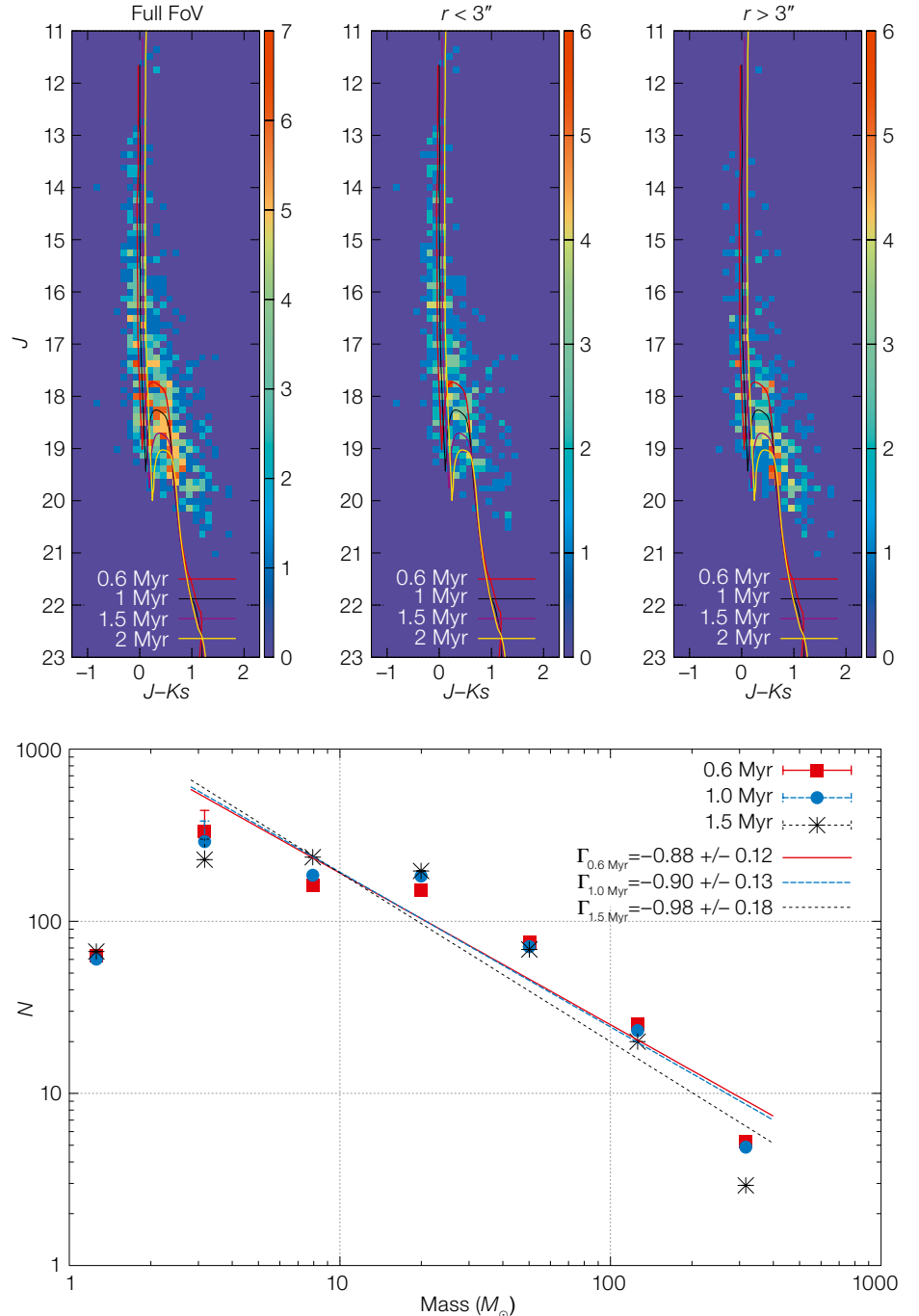
Age and extinction

To estimate the stellar ages and the extinction in the core of R136, we used the effective temperature (T_{eff}) and luminosity (log L) of 54 stars that were studied spectroscopically by Crowther et al. (2016). We also chose a grid of isochrones at different ages (from 0.1 up to 8 Myr) with the LMC metallicity ($Z = 0.006$) from the latest sets of PARSEC evolutionary models (Bressan et al., 2012), a theoretical library[1] that includes the latest set of stellar phases from pre-main sequence to main sequence and covering stellar masses from 0.1 to 350 $M_\odot$. By fitting the isochrones to each star, we estimated its age and intrinsic colour with error bars. An age range of 1.8 $^{+1.2}_{-0.8}$ Myr is the most probable for these stars. The extinction in J- and Ks-bands is 0.45 ± 0.5 and 0.2 ± 0.5 mag, respectively.

Figure 3 (upper) shows the colour-magnitude diagram (CMD) of detected sources in J- and Ks-band IRDIS data with their error bars. The CMD is plotted for the whole FoV (818 sources), in the very core of the cluster ($r < 3$ arcseconds), and outside ($r > 3$ arcseconds), from left to right. The PARSEC isochrones at four different ages (0.6, 1.0, 1.5 and 2.0 Myr) are also plotted in this figure using a distance modulus of 18.49 to R136 and central extinction values in J (0.45 mag) and K (0.2 mag).

We note that, based on the CMD isochrone fitting, ages of 1 Myr for the inner core ($r < 3$ arcseconds) and 1.5 Myr outside the core ($r > 3$ arcseconds) fit the data best. Interestingly, the age of stars in the very core ($r < 3$ arcseconds) is younger than in its outer region. This result appears to be consistent with the older population found beyond the core of R136, like the northeast clump observed by Sabbi et al. (2012), and, at a greater distance (3 arcminutes), the old cluster Hodge301, studied by Grebel & Chu (2000). In future it should be possible to understand this apparent age trend in R136, and also in the 30 Dor region, in terms of formation. Moreover, a key question is how the younger population in the centre of the cluster can be explained by star cluster formation scenarios (Wünsch et al., 2017). We note that this age differ-

ence between the two regions can also be explained by an observational bias, because the central region of R136 is very compact and bright so the incompleteness level is very low.

Considering the errors on the extinction, we can estimate the stellar mass range for each star at a given age. We estimated the stellar masses only for com-

Figure 3. Upper: Colour-magnitude diagram (CMD) in 3D showing the number density of stars. The CMD is plotted for the whole FoV (left), in the very core of the cluster ($r < 3$ arcseconds, centre) and outside ($r > 3$ arcseconds, right). Solid red, black, pink, and yellow lines depict PARSEC isochrones (corrected for distance modulus of 18.49 and central values of extinctions, $A_J = 0.45$ mag and $A_K = 0.2$ mag) at the ages of 0.5, 1, 1.5 and 2 Myr, respectively. Lower: Generalised histogram of the stellar masses (mass function, MF) at 0.6, 1 and 1.5 Myr. PARSEC models were used to estimate the stellar-mass range for each source using the extinction range.
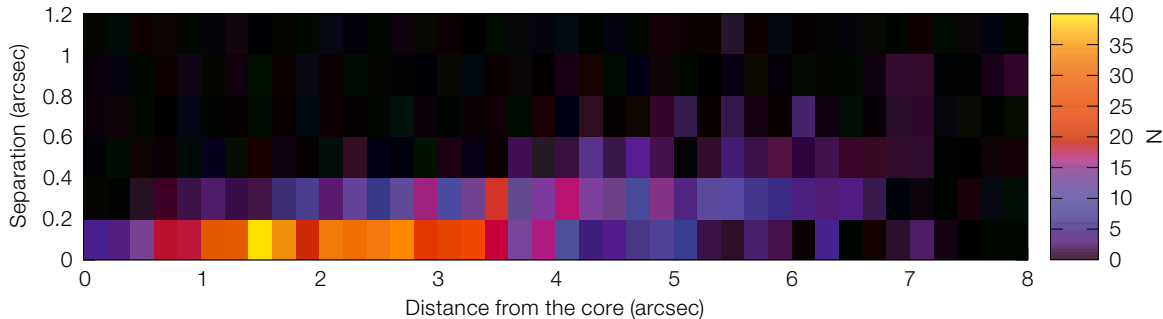
Figure 4. Histogram of the separation of the close detected sources versus their distance from the core of R136.

mon sources between *J* and *Ks* data, using their magnitudes fitted to PARSEC isochrones at three different ages: 0.6, 1, and 1.5 Myr. The histogram of mass, i.e. the mass function (MF), is plotted on the basis of a Gaussian distribution for each stellar mass. The Gaussian uncertainty in the mass of each star was accounted for when constructing the MF.

Figure 3 (lower) shows the generalised histogram of the mass (MF) at three different ages (0.6, 1, and 1.5 Myr). The MF slopes for the 1 and 1.5 Myr isochrones are $\Gamma_{1\,Myr} = -0.90 \pm 0.13$ and $\Gamma_{1.5\,Myr} = -0.98 \pm 0.18$, respectively, for the mass range of $3 - 300\,M_\odot$. These values are lower limits to the steepness because of incompleteness and the central concentration of bright stars. The derived MF is limited by the resolution of the instrument and also by the detection limit of the observation. In future, using higher angular resolution data, we may resolve binaries and low-mass stars, which affect the shape of the MF.

Visual companions

For each star detected in both *J*- and *Ks*-bands, we determined the distance between the star and its closest neighbour. Figure 4 shows the number of detected neighbouring stars in *Ks* and *J* versus their separation in arcseconds. More than 250 star pairs have a closest neighbour at a separation of less than 0.2 arcseconds. Over 90 % of massive objects (brighter than 16.7 mag in *Ks* and 15 mag in *J*) have a closest neighbour at a separation less than 0.2 arcseconds.

Figure 4 shows the separation between close-by stars versus their distance from R136a1 in the core. This figure indicates that even the sources at larger radii have close visual companions, so that the large number of close visual companions is not just an effect of 2D projection on the sky across the FoV.

The most massive stars, R136a1, R136b and R136c, have visual companions detected in the near-infrared. R136a3 is also resolved as two stars with the PSF fitting technique. Both stars of the pair have a high correlation coefficient (above 70 %) with the input PSF. The separation between the R136a3 primary and secondary is about 58.9 ± 2.1 milli-arcseconds, which is larger than the FWHM of the PSF. We note that even the closest visual companions, like R136a3, are physically distant from each other (0.059 arcseconds corresponds to 2890 au). This visual separation implies a period of more than 10^4 yr for a binary system, so that these sources are probably not gravitationally bound to each other.

Future prospects

Using SPHERE data, we have gone one step further and partially resolved the core of R136, but this is certainly not the final step. R136 needs to be observed in the future with higher resolution, such as with the Extremely Large Telescope (ELT) and the James Webb Space Telescope (JWST) over a wide wavelength range (and field of view). JWST, while more sensitive than our VLT observations, will remain confusion-limited in the core. However, it will provide sensitive observations from 1–28 µm, over a field of several square arcminutes, enabling us to place the R136 cluster in context. The ELT, with its enhanced spatial resolution, will be our best chance to resolve the core, assess the low-mass end of the initial mass function (IMF), and put models of dynamical evolution to serious test. This future work may help us understand massive star formation, the impact massive stars have on their environment, and, ultimately, the formation and evolution of massive star clusters as possible sites for the emergence of stellar black hole binaries whose mergers have recently been detected as sources of gravitational waves.

References

Beuzit, J.-L. et al. 2008, SPIE, 7014, 701418
Bressan, A. et al. 2012, MNRAS, 427, 127
Campbell, B. et al. 1992, AJ, 104, 1721
Campbell, M. A. et al. 2010, MNRAS, 405, 421
Cassinelli, J. P., Mathis, J. S. & Savage, B. D. 1981, Sci, 212, 1497
Grebel, E. K. & Chu, Y.-H. 2000, AJ, 119, 787
Crowther, P. A. et al. 2010, MNRAS, 408, 731
Crowther, P. A. et al. 2016, MNRAS, 458, 624
Diolaiti, E. et al. 2000, A&AS, 147, 335
Feitzinger, J. V. et al. 1980, A&A, 84, 50
Hunter, D. A., Shaya, E. J. & Holtzman, J. A. 1995, ApJ, 448, 179
Khorrami, Z. et al. 2016, A&A, 588, L7
Langlois, M. et al. 2014, SPIE, 9147, 91479P
Sabbi, E. et al. 2012, ApJ, 754, L37
Savage, B. D. et al. 1983, ApJ, 273, 597
Weigelt, G. & Baier, G. 1985, A&A, 150, L18
Wünsch, R. et al. 2017, ApJ, 835, 60

Links

[1] PARCSEC evolutionary models: http://stev.oapd.inaf.it/cgi-bin/cmd